Hall Effect in Oriented Single Crystals of *n*-Type Germanium*

W. M. BULLIS† AND W. E. KRAG
Lincoln Laboratory, Massachusetts Institute of Technology, Lexington, Massachusetts
(Received September 22, 1955)

Hall measurements have been made on oriented single crystals of n-type germanium confirming the variations of the Hall coefficient with the direction and magnitude of the magnetic field, and with the direction of the current, which are predicted by theories based on the eight-ellipsoid model. Although other assumptions must be made to secure exact agreement, these measurements, when made under suitable conditions, can be explained by a theory assuming an energy-independent scattering time τ. This type of measurement may be useful in determining symmetry properties of the energy surfaces near a band edge in other semiconductors.

I. INTRODUCTION

THEORETICAL calculations[1,2,3] based on the eight-ellipsoid model for the conduction band of germanium indicate that the Hall coefficient varies with the orientation and magnitude of the magnetic field and with the orientation of the current. These variations depend on both the scattering mechanism and the structure of the conduction band near the edge of the energy gap. Since the eight-ellipsoid model for n-type germanium has been well established by cyclotron resonance measurements,[4] differences between theoretical calculations and experimental results may be attributed to the assumption made concerning the scattering mechanism.

In this paper it is shown that calculations using an energy-independent mean free time, τ, yield results which agree reasonably well with experimental data taken at 77°K on n-type germanium.[5] The samples measured had an impurity concentration of about 1.6×10^{14} cm^{-3} so that the holes did not contribute significantly to the current at this temperature—a necessary restriction since the theories are derived on the basis of a single type of carrier.

II. THEORY AND CALCULATIONS

The normal Hall coefficient can be defined as

$$R_H=\mathbf{E}\cdot(\mathbf{J}\times\mathbf{B})/(\mathbf{J}\times\mathbf{B})^2, \tag{1}$$

where $\mathbf{E}$ is the total electric field in the crystal, $\mathbf{J}$ is the current density, and $\mathbf{B}$ is the magnetic field. By substituting $\rho\mathbf{J}$ for $\mathbf{E}$ in this definition, the Hall coefficient can be expressed in terms of elements of the resistivity tensor, ρ.[6] Assuming that the surfaces of constant energy are also surfaces of constant mean free time, and that Boltzmann statistics apply, the elements of this tensor can be expressed in terms of integrals[7] of the following type:

$$I_n=\int_0^\infty \frac{\tau^n\epsilon^{\frac{3}{2}}e^{-\epsilon/kT}d\epsilon}{1+w^2\tau^2}, \tag{2}$$

where $n=1$, 2, or 3; τ is the mean free time; k is the Boltzmann constant; T is the absolute temperature; ϵ is the energy; and w is a function of the magnetic field $\mathbf{B}$ and of K, the ratio of the longitudinal mass m_l to the transverse mass m_t.

The assumption of an energy-independent mean free path[8] leads directly to the results of Abeles and Meiboom[1] or Shibuya[2] and the assumption of an energy-independent mean free time leads to results identical with those obtained by Gold and Roth.[3] For an energy-independent mean free time the integrals, and therefore the Hall coefficient, may be calculated as a function of a variable: $b=b_\tau=eB\tau/m_tc$, where e is the electronic charge and c is the velocity of light. Since the Hall coefficient depends only slightly on the value of the mass ratio, K, comparisons with experimental data can be made merely by expanding or compressing the b scale. The situation for an energy independent mean free path is generally more complicated and the calculations must be made separately for each value of the Hall mobility.[8] This, together with the fact that the calcula-

* The research in this document was supported jointly by the Army, Navy, and Air Force under contract with the Massachusetts Institute of Technology.

† On educational leave from the Diamond Ordnance Fuze Laboratories, Washington, D. C.

1 B. Abeles and S. Meiboom, Phys. Rev. **95**, 31 (1954).

2 M. Shibuya, Phys. Rev. **95**, 1385 (1954).

3 L. Gold and L. Roth (to be published).

4 Lax, Zeiger, Dexter, and Rosenblum, Phys. Rev. **93**, 1418 (1954); Lax, Zeiger, and Dexter, Physica **20**, 818 (1954); Dresselhaus, Kip, and Kittel, Phys. Rev. **98**, 368 (1955).

5 *Note added in proof.*—This mean free time is not intended to represent a physical process but rather is used as a mathematical convenience which is valid over a range of experimental conditions where the total scattering time is not a strong function of the energy.

6 Such as those described in reference 2.

7 These integrals may be derived in the manner described in reference 1 if the explicit energy dependence of τ is omitted. The integrals I_1, I_2, and I_3 are equivalent to the expressions α, β, and γ, respectively, as defined in Eqs. (4.5)–(4.7) of reference 1. The conductivity tensor S_{ik} may be described in the general case if, in Eqs. (4.11) and (4.12) of reference 1, $u=2^{\frac{1}{2}}e^2m_t/3\pi^2\hbar^3m_e^{\frac{1}{2}}$, $v=e/m_lc$, $\alpha\rightarrow I_1$, $\beta\rightarrow I_2$, $\gamma\rightarrow I_3$, and the expression w for each family of ellipsoids is given by a w_j. Equations (4.13) remain unchanged. The procedure for determining the coefficients for specified directions is outlined immediately following these equations in reference 1.

8 In the case of ellipsoidal energy surfaces this assumption gives a scattering time $\tau=l\epsilon^{-\frac{1}{2}}$, where the mean free path, l, is isotropic and independent of energy. If l is not isotropic, the mass ratio, K, also includes a factor due to the anisotropy of l (compare reference 1). The Hall mobility, $\mu_H=R_0\sigma_0$, is usually used as the parameter for this assumption instead of the mean free path.

tions are numerically much more complex, makes comparison with experimental data difficult. However, in the case where **B** is in a ⟨100⟩ direction and **J** is perpendicular to **B**, the integrals and the Hall coefficient may be calculated as a function of a variable:

$$b=b_l=\frac{el}{m_t}\left(\frac{K+2}{3K}\right)^{\frac{1}{2}}\frac{1}{(kT)^{\frac{1}{2}}}B=\frac{2}{(\pi)^{\frac{1}{2}}}\frac{(2K+1)}{[3K(K+2)]^{\frac{1}{2}}}\mu_H B.$$

Since the variation with K is very slight, comparisons with experimental data can be made in the same fashion as for the energy independent mean free time case.

As has been noted elsewhere[2,9] the Hall coefficient for an infinite magnetic field, R_∞, is equal to $(Nec)^{-1}$, where N is the total electron concentration, irrespective of the orientation of **B** or **J**, the mass ratio, and the mean free time. Therefore, it is convenient to normalize the Hall coefficient to its limit for $B=\infty$.

Calculations of the Hall coefficient as a function of b_τ or b_l for a number of cases are plotted in Fig. 1. Curves 1 to 4 are for the case where **B** is along a cubic axis and **J** is perpendicular to the axis. Curves 1 and 2 were calculated from $R_{100}{}^{010}$, Eq. (4.14), of Abeles and Meiboom[1] ($b_l=\xi$ in their notation) for $K=17.4$ and $K=19$, respectively. (The latter value of K is that obtained from cyclotron resonance measurements[4] at 4.2°K.) Curves 3 and 4 were calculated from the equation[10]

$$\frac{R_H}{R_\infty}=\frac{3K(K+2)}{(2K+1)^2}\frac{m}{1+z^2b^2}, \tag{3}$$

where $m=1+(K+2)b^2/3K$ and $z=(K+2)/(2K+1)$, for $K=16.9$ and $K=19$, respectively. Curves 5 and 6, for which **B** is in a ⟨110⟩ direction and **J** is in a ⟨100⟩ or ⟨1$\bar{1}$0⟩ direction, were calculated from the equation

$$\frac{R_H}{R_\infty}=\frac{3K(K+2)}{(2K+1)^2}\frac{[2m-1+qb^4][1-(xb^2/2z)]}{m[1-\frac{1}{2}xb^2+z^2b^2-xzb^4+\frac{1}{4}x^2b^6]}, \tag{4}$$

where $x=n(K-1)/m(2K+1)$, $n=2(K-1)/3K$, $q=(2K+1)/3K^2$, and $2m-1+qb^4=m^2-\frac{1}{4}n^2b^4$, for $K=16.9$ and $K=19$, respectively. Curve 7, for which both **B** and **J** are along the same cubic axis, was calculated from the equation

$$\frac{R_H}{R_\infty}=\frac{3K(K+2)}{(2K+1)^2}\frac{m[1+yb^2+xb^2(z-1)/z]}{(1+yb^2)(1+z^2b^2)}, \tag{5}$$

where $y=3/(2K+1)$, for $K=19$. Although this last case cannot be measured experimentally since the Hall voltage is zero, the group of curves 4, 6, and 7 gives an idea of the variation of the Hall coefficient as the

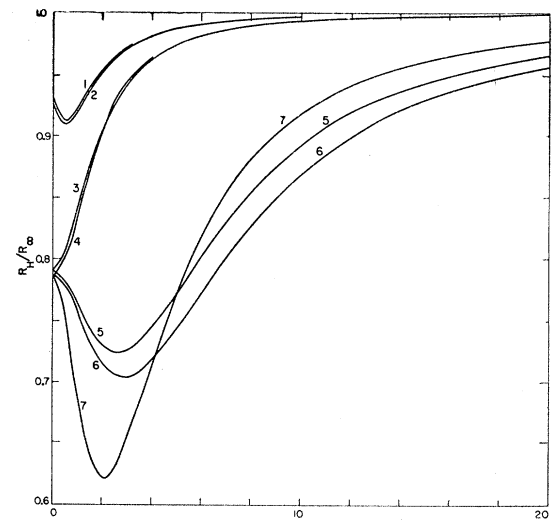

FIG. 1. Hall coefficient *vs* b. The abscissa for curves 1 and 2 is b_l (energy-independent mean free path) and for the remainder of the curves is b_τ (energy-independent mean free time). For curves 1 to 4, **B** is along a cubic axis and **J**⊥**B**; for curves 5 and 6, **B** is along a ⟨110⟩ axis and **J** is along a ⟨100⟩ or ⟨1$\bar{1}$0⟩ axis; for curve 7, **J** and **B** are along the same cubic axis. For curves 3 and 5, $K=16.9$; for curve 1, $K=17.4$; and for curves 2, 4, 6, and 7, $K=19$.

magnetic field **B** is rotated in a plane perpendicular to the cubic axis along which the Hall field is measured and including the cubic axis along which the current flows.

The Hall coefficient for zero field, R_0, is also independent of the orientation of **B** and **J**. Assuming that the mean free time depends on energy as $\tau=\lambda\epsilon^\gamma$, where λ is independent of energy, it can be shown that

$$\frac{R_0}{R_\infty}=\frac{3K(K+2)}{(2K+1)^2}\frac{\Gamma(5/2+2\gamma)\Gamma(5/2)}{\Gamma^2(5/2+\gamma)}=F(K)G(\gamma). \tag{6}$$

It is seen that R_0 is quite insensitive to the mass ratio for moderately large values ($K\gtrsim 10$).[11] The expression $G(\gamma)$, shown in Fig. 2, indicates the dependence of R_0 on the scattering mechanism.

Calculations of the Hall coefficient as a function of θ, the angle between the current and the magnetic field, can be made if the mean free time is assumed to be energy independent. For **B** in the (001) plane the Hall coefficient for **J** in the [100] direction is given by[10]

$$\frac{R_H}{R_\infty}=\frac{3K}{2K+1}\frac{m^2-n^2b_1{}^2b_2{}^2}{m}\frac{N(b_1,b_2)}{D}, \tag{7}$$

and the Hall coefficient for **J** in the [110] direction is given by

$$\frac{R_H}{R_\infty}=\frac{3K}{2K+1}\frac{m^2-n^2b_1{}^2b_2{}^2}{m}\frac{\beta_2N(b_1,b_2)-\beta_1N(b_2,b_1)}{(\beta_2-\beta_1)D}. \tag{8}$$

[9] C. Herring, Bell System Tech. J. 34, 237 (1955).

[10] Equations (3), (4), (5), (7), and (8) may be calculated from the integrals, Eq. (2), in the manner described in reference 7 assuming that τ is energy-independent, or they may be calculated by the method of reference 3. The authors are indebted to Dr. Gold for the calculations of curves 3 and 5 of Fig. 1 [Phys. Rev. 99, 596 (1955)].

[11] The expression $F(K)$ is shown in Fig. 1, reference 1.

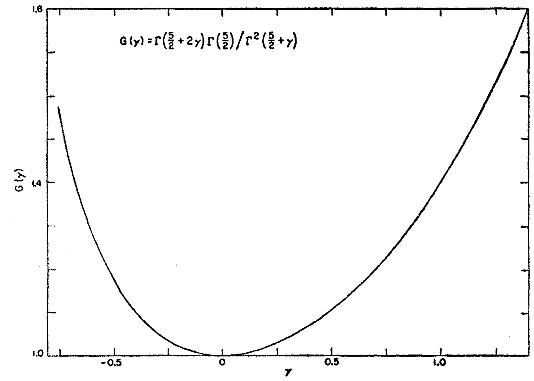

FIG. 2. $G(\gamma)$ *vs* γ showing the variation of the zero-field Hall coefficient, R_0, with the energy dependence of τ, assuming $\tau=\lambda\epsilon^{\gamma}$. The curve gives an idea of the dependence of R_0 on the scattering mechanism.

In these equations: m, n, x, y, and z are as defined above;

$$N(b_i,b_j)=(x+y)b_i^2(z-xb_j^2)+(z-xb_i^2)(1+yb_j^2);$$

$$D=\{(1+yb^2)(1+z^2b^2)+xb^4\beta_1^2\beta_2^2[(x+2y)(1+2zb^2)-2z(z-2)-xb^2]+2x^2b^8\beta_1^4\beta_2^4(x+2y)\};$$

$b_1=b\beta_1$, $b_2=b\beta_2$, and β_1 and β_2 are the direction cosines of **B** with respect to the [100] and [010] axes respectively. Curves for a number of cases are plotted in Fig. 3.

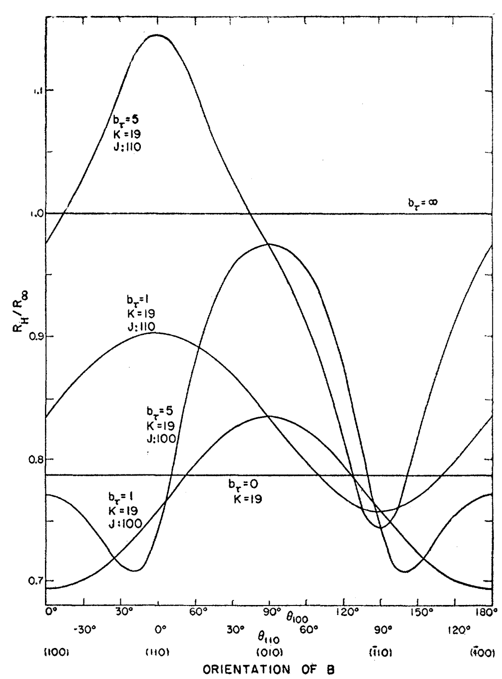

FIG. 3. Hall coefficient *vs* angle θ calculated from Eqs. (7) and (8) for various values of b_τ and for $K=19$. For $b_\tau=0$ and $b_\tau=\infty$ the coefficient is independent of the orientation of the current as well as the orientation of the field. The abscissa gives values of θ for both directions of current for which calculations were made. Cardinal directions of **B** are also given.

III. EXPERIMENTAL TECHNIQUES

The Hall coefficient is determined experimentally by measuring the Hall voltage for the four conditions obtained by reversing separately the current and the magnetic field, averaging these measured voltages to eliminate even functions of **J** and **B**, and putting this averaged voltage, V_H, in the formula

$$R_H=V_Ht/IB\sin\theta, \tag{9}$$

where I is the current, t is the thickness of the sample in a direction perpendicular to both the current and the Hall field, and θ is the angle between the current and the magnetic field. The reason for this procedure is that the even functions of **J** and **B** are unwanted as they arise in general from thermal effects and from the IR drop between the Hall leads.[12] However, for orientations

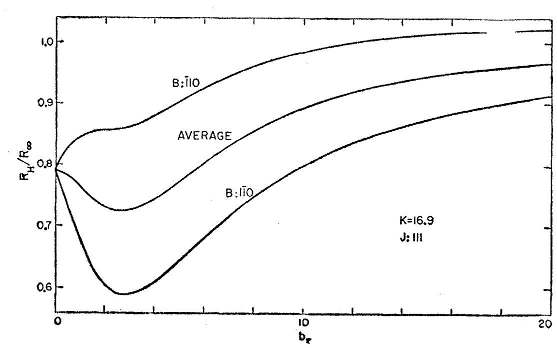

FIG. 4. Hall coefficient *vs* b, calculated for a less highly symmetric orientation showing the changes with reversal in magnetic field. The "average" curve is obtained by eliminating that part of the Hall voltage which is an even function of **B**, thus retaining only the antisymmetric part of the resistivity tensor. The calculations are due to L. Gold (unpublished).

which are not highly symmetric, there are true contributions to the Hall voltage, as it is defined here, arising from symmetric parts of the resistivity tensor which are even functions of **B**. Since the definition of the Hall coefficient given above considers the total transverse voltage as the Hall voltage, it is necessary to eliminate the even, or symmetric, terms from the theoretical calculations when making comparison with experimental data for the less highly symmetric orientations.[13] A theoretical calculation for such a case is shown in Fig. 4.

The measurements were made on oriented samples cut from a single crystal of antimony doped germanium. The samples were rectangular parallelepipeds about 20 mm long, 4 to 8 mm wide and 2 mm thick. The surfaces were sandblasted and leads were attached with Cerroseal

[12] Except for the Ettinghausen effect; see, for example, O. Lindberg, Proc. Inst. Radio Engrs. **40**, 1414 (1952).

[13] Herring (reference 9) considers the Hall coefficient as being derived solely from the antisymmetric parts of the resistivity tensor. This definition emphasizes the coefficient and avoids any difficulty in comparing with data averaged as above. The definition in this paper considers the transverse (Hall) voltage as fundamental rather than the coefficient.

solder. The current contacts completely covered the ends of the sample. Potential contacts, about 0.5 mm in diameter, were soldered to both sides of the sample about 7 mm from each end providing two simultaneous measurements of the Hall voltage. The current always flowed along the long axis which was either a ⟨100⟩ or a ⟨110⟩ crystal axis. The Hall voltage was measured across the width of the sample which was always in an ⟨001⟩ direction. The sample was mounted on a holder which was immersed in a Dewar flask containing liquid nitrogen and could be rotated through 360 degrees. Since the sample was in contact with the boiling liquid nitrogen thermal effects were negligible. The temperature of the boiling liquid was monitored by means of copper-constantan thermocouple and was constant to within 0.1°C.

Uniform magnetic fields up to 20 000 gauss were provided by a Varian 12-in. electromagnet and were measured with a nuclear resonance magnetometer. All potentials were measured with a Rubicon Type B potentiometer. The sample current, which remained essentially constant during a sequence of measurements, was determined at regular intervals by measuring the potential drop across a series resistor. The Hall voltage was found to be proportional to the current over the range observed, which included currents from 0.1 to 5 milliamperes. Distortion effects[14] due to shorting of the sample ends by the conducting solder were shown to be negligible by repeating some of the measurements after the sample had been cut in half along the long axis.

IV. EXPERIMENTAL RESULTS

A. Hall Coefficient *Versus* Field Strength

Measurements of the Hall coefficient as a function of magnetic field were made at 77°K for a number of orientations. The high symmetry orientations, which are most convenient to measure, can be grouped into a number of classes. Several typical curves are shown in Fig. 5 together with the theoretical curves calculated using an energy independent mean free time. The horizontal scales of these curves are fitted so that the abscissas of the minimas of the experimental curves B and theoretical curve 6 in Fig. 1 coincide. Thus an effective value for τ can be calculated. For the samples measured, $\tau \approx 2.4 \times 10^{-12}$ sec. It can be seen that the theoretical curves have the same shape as the experimental even though there are quantitative differences. If the experimental results are extrapolated, the value of the Hall coefficient at $B=0$ thus obtained can be fitted by putting $\gamma \approx -0.24$ in Eq. (6). Computations using this value of γ have not been carried out for finite fields due to their numerical complexity and the quantitative inadequacy of the simple power law assumption. It is not possible to fit the extrapolated curves at $B=0$ by varying only K. The value of R_∞ is determined by plotting the Hall coefficient as a function of $1/B^2$ and extrapolating linearly to the value of $B=\infty$ as shown in Fig. 6. For curves from this crystal which could not be extrapolated in this fashion, the extrapolation was made to $B=0$ and the ratio R_0/R_∞ as found from curve A in Fig. 5 was assumed to be correct.

[14] R. F. Wick, J. Appl. Phys. 25, 741 (1954).

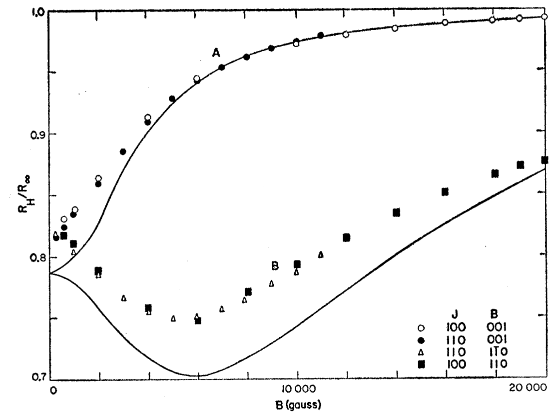

FIG. 5. Hall coefficient *vs* magnetic field. The experimental results are grouped into the two classes: (A) where $\mathbf{B}$ is in an ⟨001⟩ direction and $\mathbf{J}$ is in the {001} plane and (B) where $\mathbf{B}$ is in a ⟨110⟩ direction and $\mathbf{J}$ is in a ⟨100⟩ or ⟨$1\bar{1}0$⟩ direction. The solid curves are the theoretical curves 4 and 6 of Fig. 1 with $\tau = 2.4 \times 10^{-12}$ sec, $b_\tau = 5 \times 10^{-4} B$.

B. Hall Voltage *Versus* Angle θ

The Hall voltage was measured as a function of the angle θ between $\mathbf{J}$ and $\mathbf{B}$. The current direction and field strength were held constant and $\mathbf{B}$ remained in the {001} plane. The results for $B=2000$ gauss are shown in Fig. 7, and the results for $B=10\,000$ gauss are shown in Fig. 8 together with theoretical curves calculated using the

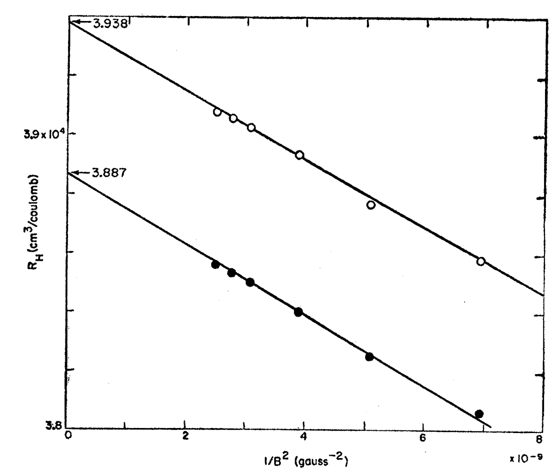

FIG. 6. Hall coefficient *vs* $1/B^2$. The 1.3% difference between these two measurements which were taken simultaneously at different points on the same sample indicates the limit of the absolute accuracy of these measurements. This difference may be due to differences in impurity concentration and/or to slight variations in the dimensions of the sample. When $B=\infty$, $R_H = (Nec)^{-1}$.

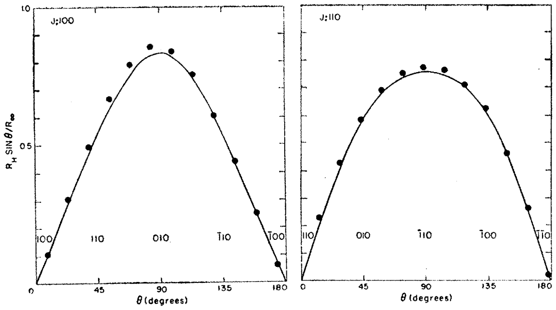

FIG. 7. Hall voltage *vs* angle θ for $B=2000$ gauss. The points are experimental and the solid curves were calculated assuming an energy-independent τ with $b_\tau=1$, $K=19$. Cardinal directions of **B** are shown for each case.

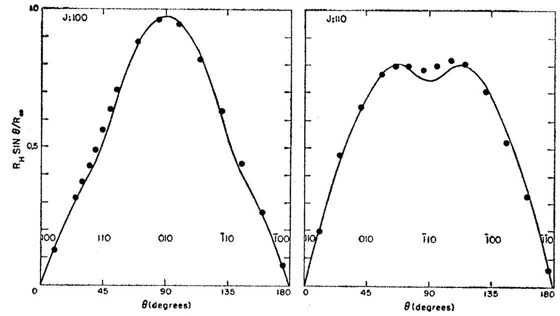

FIG. 8. Hall voltage *vs* angle θ for $B=10\,000$ gauss. The points are experimental and the solid curves were calculated assuming an energy independent τ with $b_\tau=5$, $K=19$. Cardinal directions of **B** are shown for each case.

value of τ determined above. The curves are presented with the ordinate $R_H \sin\theta/R_\infty$ (proportional to the Hall voltage) rather than R_H/R_∞ because of the uncertainty in the value of θ which is known only to about a degree. The zero for the θ scale was placed at the point where the Hall voltage was zero. The measurements are sufficiently accurate to show that the agreement is not exact but it can be seen that the general features of the curves are in excellent agreement.

V. CONCLUSIONS

It has been shown that the experimental results can be explained by a theory based on an energy-independent mean free time, τ, which thus becomes a parameter by which it is possible to relate experimental results to theoretical calculations over a reasonably wide range of experimental conditions where the energy dependence of the scattering time is not very strong. This results in a qualitative separation of the properties due to the scattering mechanism and those due to the band structure of the material which suggests that it is possible to apply this type of measurement to determine the symmetry properties of the band structure near the band edges on materials for which the more direct cyclotron resonance measurements are not now possible. The method described here is restricted to materials whose band structures can be represented by "simple" or "simple many-valley" models for the energy surfaces[15] and may not be applicable to materials with degenerate energy surfaces such as *p*-type germanium and *p*-type silicon.

Since the measurements described above are relatively insensitive to the value of the mass ratio, K, the information obtained from them is not really complete. However, if the restrictions of Eq. (2) apply, the infinite-field limit of the longitudinal magnetoresistance coefficient is a function only of K.[8] For any arrangement of the valleys in the simple many-valley model there will be an optimum direction in which the limiting value of this magnetoresistance coefficient will depend most strongly on K. Coupling this measurement with the Hall measurements will therefore yield the complete solution provided that the assumptions made are adequate. Experiments are now in progress to determine the validity of these assumptions and will be reported in the near future.

VI. ACKNOWLEDGMENTS

The authors wish to acknowledge the support and encouragement of Dr. Benjamin Lax who originally proposed the problem. They are indebted to Professor J. E. Thomas, Jr., for his support, to other members of the Solid State Group for their assistance in preparing and orienting the samples and making preliminary measurements, and to Miss M. C. Glennon for her help with some of the calculations. Particular thanks are due Professor W. P. Allis for many helpful suggestions and discussions and Dr. L. Gold for many discussions including discussions of his work prior to publication.

[15] As defined by Herring (reference 9).